

International Congress on Ultrasonics, Universidad de Santiago de Chile, January 2009

## Evaluation of the influence of large temperature variations on the grey level content of B-Mode images

André V. Alvarenga<sup>a\*</sup>, César A. Teixeira<sup>b</sup>, Maria Graça Ruano<sup>b</sup>, Wagner C. A. Pereira<sup>c</sup>

<sup>a</sup>Laboratory of Ultrasound/National Institute of Metrology, Standardization and Industrial Quality (Inmetro), Duque de Caxias, Brazil

<sup>b</sup>Centre for Intelligent Systems/University of Algarve, Faro, Portugal

<sup>c</sup>Biomedical Engineering Program/COPPE, Federal University of Rio de Janeiro, Rio de Janeiro, Brazil

---

### Abstract

In this work, the variation of the grey-level content of B-Mode images is assessed, when the medium is subjected to large temperature variations. The goal is to understand how the features obtained from the grey-level pattern can be used to improve the actual state-of-the-art methods for non-invasive temperature estimation (NITE). Herein, B-Mode images were collected from a tissue mimic phantom heated in a water bath. Entropy was extracted from image Grey-Level Co-occurrence Matrix, and then assessed for non-invasive temperature estimation. During the heating period, the average temperature varies from 27°C to 44°C, and entropy values were capable of identifying variations of 2.0°C. Besides, it was possible to quantify variations in the range from normal human body temperature (37°C) to critical values, as 41°C. Results are promising and encourage us to study the uncertainty associated to the experiment trying to improve the parameter sensibility.

*Keywords:* Non-invasive temperature estimation; grey-level content; image processing techniques; ultrasound.

---

### 1. Introduction

It is of common sense that the existence of reliable temperature estimators could improve the security and effectiveness of thermal therapies. In the most direct attempt, temperature can be assessed invasively, i.e. by direct measurement at the treatment site. However, tissue damage and, in some situations, the impossibility to adequately place sensors raise the necessity to look for non-invasive methods. Non-invasive temperature estimation (NITE) methodologies are based on the extraction of temperature-dependent features from available signals. A technology that could bring some advantages in obtaining such signals is ultrasound. Based on backscattered ultrasound, four features have been claimed to have potential for NITE in literature. These features are: medium attenuation coefficient [1], time-shifts (TS) [2], spectral component shifts [3], and backscattered energy [4]. Among these features, the one that has been receiving special attention is TS, because it is declared to be a monotonic function of temperature, and it is also intrinsically independent of the transducer on usage. Theoretical and experimental studies

---

\* Corresponding author. Tel.: +55-21-2679-9720; fax: +55-21-2679-1296.

E-mail address: [avalvarenga@inmetro.gov.br](mailto:avalvarenga@inmetro.gov.br).

were performed and consistent results were obtained for temperature variations up to 10°C [2,3]. Previous reported models based on TS were built from linear relationships. More recently, a non-linear methodology, also based on TS, was proposed for NITE presenting a higher performance at both error and operational levels [5]. A drawback of this methodology is that it estimates temperature at discrete spatial points. It is then necessary to complement it to perform continuous-space estimates. It is envisaged that the addition of image processing information to the non-linear technique could then result in improved continuous-space maps.

This paper explores the potentiality of an image texture parameter in quantifying medium temperature variation. B-Mode ultrasound images were collected while a phantom was heated. The performance of the parameter entropy, calculated from Grey-Level Co-occurrence Matrix (GLCM), was then assessed.

## 2. Experimental Set-up

The experimental set-up developed is presented in Fig. 1. The phantom heating system is composed by two Pyrex Beakers. The smaller (1000 ml) contains the phantom. The bigger one (2000 ml) contains degassed water and acts like a thermal capacitor, avoiding brusque temperature changes and improving uniform phantom heating. Temperature elevation is obtained by using a common laboratory heater.

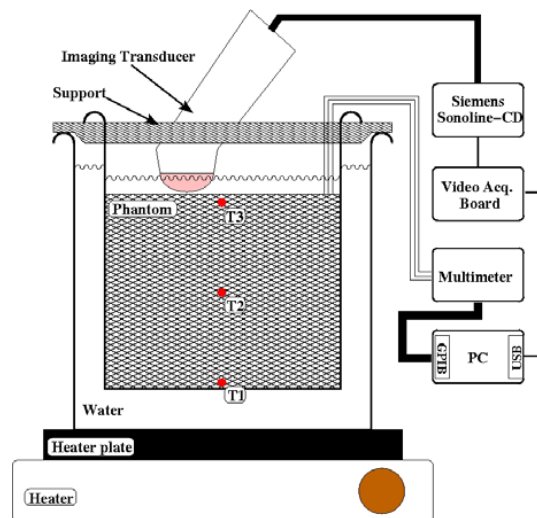


Fig.1 Experimental set-up. T1, T2 and T3 are thermocouples.

The tissue mimic material placed inside the 1000 ml beaker is a mixture (in % of weight) of: 86.5 % of water, 11 % of glycerine and 2.5 % of agar-agar. Graphite powder (equivalent to 1 % of the water weight) is added to the mixture to obtain acoustic backscattered information from the medium. This mixture is basically the one presented in [6], which has acoustical properties similar to human soft tissue.

Temperature was acquired by three thermocouples placed inside the phantom. The first one (T1) was placed close to the bottom of the smaller beaker; a second one (T2) was placed in the middle of the phantom. The third thermocouple was put at the top of the phantom, *i.e.*, close to the transducer. The thermocouples were connected to a cold junction compensated multiplexer, which is part of a digital multimeter (2700/7700, Keithley). The temperature values are sent to a PC via a GPIB interface at each 10 s.

The B-Mode images used in this study are acquired by a commercial imaging ultrasound system (IUS) (Siemens, Sonoline CD), which has a mechanical sector transducer (3.5 MHz), thus producing sector images. The video output

of the IUS system was connected to a USB video acquisition board (DVD EZMaker USB Plus, Avermedia) that enabled the recording of the B-Mode images (25 frames/s). An example of a collected B-Mode image, as well as the temperature along an experiment trial, is presented in Fig. 2.

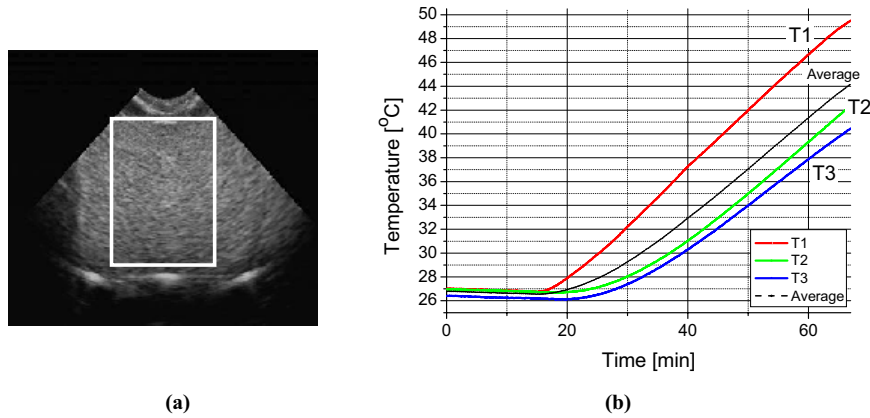


Fig.2 Measured data. (a) Example of a B-Mode image. The region of interest (ROI) including the three thermocouples is represented by the white rectangle. (b) Temperature curves for thermocouples T1, T2 and T3; the dashed line represents the average temperature.

### 3. Texture Features

The GLCM is a bi-dimensional histogram ( $G \times G$ ) of elements  $p(i,j)$ , defined as the number of pixel-pairs  $(i,j)$  occurrences for which a grey-level  $i$  is spaced out of a grey-level  $j$  by a distance  $d$ , and along a direction  $\theta$  [7]. Herein, to avoid sparse GLCMs (low populated classes), the number of grey-levels was reduced to 32 resulting in matrix size of  $32 \times 32$ , and a three-pixel distance ( $d = 3$ ) was chosen. In addition, to avoid possible bias due to the direction ( $\theta$ ) chosen, the average of four matrices, each one obtained for a different direction ( $\theta = 0^\circ, 45^\circ, 90^\circ$  and  $135^\circ$ ), was used. This averaged matrix was normalised by the total number of pixels before calculating the texture features. In this work, the entropy of GLCM is defined in (1), in accordance to [8].

$$entropy = \sum_{i,j} p(i,j) \cdot \log[p(i,j)] \quad (1)$$

### 4. Data pre-processing

A region of interest (ROI) containing the three thermocouples and surroundings was manually selected (Fig. 2a). For each region, GLCM features were calculated for all frames, during the entire process of heating. Entropy was calculated for each 250 frames (corresponding to 10s) and then averaged, furnishing one single entropy value to each read temperature. In addition, the temperature values measured from the three thermocouples were also averaged to represent the temperature of the ROI.

### 5. Results and Discussion

During the initial fifteen minutes, average temperature presented an almost imperceptible decreasing, and entropy values seem to slightly decrease (Fig. 3). However, entropy values and temperature presented just a moderate correlation (Table 1). Besides, temperature variation was not considered significant, once it occurs on hundredths of

degree Celsius (below thermocouple nominal precision). When temperature started to increase, entropy values started to increase too, presenting a high correlation (0.95) between them (Table 1).

The scatter plot of temperature versus entropy values, as well the respective fitted curve, are presented in Fig. 4. Assessing this fitted curve, and its respective error range (dashed lines), one can observe that it seems to be possible to estimate temperature variations of  $2.0^{\circ}\text{C}$  (arrows at  $28.0^{\circ}\text{C}$ ,  $30^{\circ}\text{C}$  and  $32^{\circ}\text{C}$  in Fig. 4) using entropy values. Moreover, it was possible to quantify the variation from the normal human body temperature ( $37^{\circ}\text{C}$ ) to critical values, as  $41^{\circ}\text{C}$  (two arrows on the right in Fig. 4).

As the heater plate is positioned on the phantom bottom, heat tends to propagate progressively towards the phantom top. Thus, as it can be observed on Fig. 2b, the farther is the thermocouple from the heater, the slower is the temperature growth. This behaviour is associated to the natural heating process of the medium, respecting its local particularities. Moreover, it is worth emphasizing that this phenomenon seems to be also captured by the entropy dispersion during the phantom-heating period (Fig. 3).

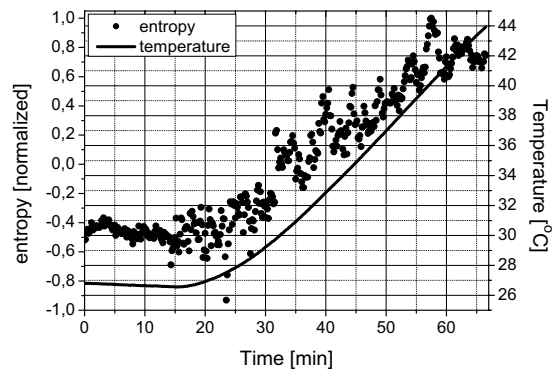


Fig.3 Behaviour of entropy and temperature during the whole experiment cycle.

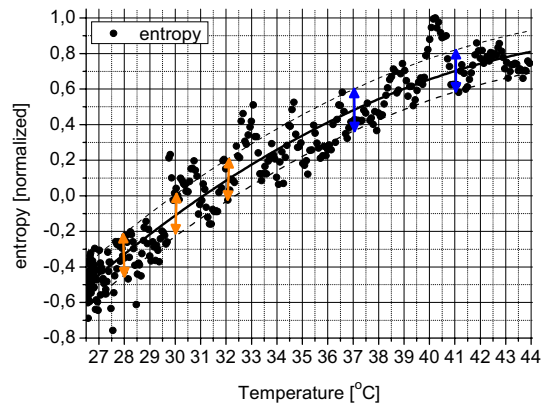


Fig.4. Entropy variation versus temperature. The solid line represents the fitted function, while dashed lines represent its error range. The three arrows to the left point out variations of  $2^{\circ}\text{C}$ , while the two arrows to the right show entropy variation from normal human body temperature ( $37^{\circ}\text{C}$ ) to critical values, as  $41^{\circ}\text{C}$ .

Table 1. Values of correlation between entropy and temperature in different periods of the experiment.

Parameter	Correlation	
	0 – 15 min	15 – 70 min
<i>entropy</i>	0.50	0.95

## Conclusion

In this paper, the entropy, calculated from Grey-Level Co-occurrence Matrix, extracted from B-Mode images was assessed for non-invasive temperature estimation in a tissue mimic phantom heated by a laboratory heater. During the heating period, the average temperature varies from 27°C to 44°C, and entropy values were capable of identifying variations of 2.0°C. Besides, it was possible to quantify variations in the range related to human body temperature (37 - 41°C). Results are promising and encourage us to study the uncertainty associated to the experiment trying to improve the parameter sensibility. Furthermore, it is expected that with farther research, image-processing information could be a useful complement to the existent estimation methodologies, resulting in improved temperature maps.

## Acknowledgements

The authors would like to thank: Fundação para a Ciência e a Tecnologia (grant SFRH/BD/14061/2003 and project POSC/EEA-SRI/61809/2004), Portugal; Conselho Nacional de Desenvolvimento Científico e Tecnológico (CNPq), and FAPERJ (E-26/170.597/2007 - APQ5) Brazil.

## Reference

- [1] S. Ueno, M. Hashimoto, H. Fukukita, and T. Yano, "Ultrasound thermometry in hyperthermia," Proc. IEEE Ultrasonics Symposium, vol. 3, pp. 1645-1652, 1990.
- [2] C. Simon, P. Van Baren, and E. S. Ebbini, "Two-dimensional temperature estimation using diagnostic ultrasound," IEEE Trans. Ultrason., Ferroelect., Freq. Contr., vol. 45, pp. 1088-1099, 1998.
- [3] A. N. Amini, E. S. Ebbini, and T. T. Georgiou, "Noninvasive estimation of tissue temperature via high resolution spectral analysis techniques," IEEE Trans. Biomed. Eng., vol. 52, pp. 221-228, 2005.
- [4] R. M. Arthur, W. L. Straube, J. D. Starman, and E. G. Moros, "Noninvasive temperature estimation based on the energy of backscattered ultrasound," Med. Phys., vol. 30, pp. 1021-1109, 2003.
- [5] C. A. Teixeira, M. G. Ruano, A. E. Ruano, and W. C. A. Pereira, "A soft-computing methodology for non-invasive time-spatial temperature estimation," IEEE Trans. Biomed. Eng., vol. 22, pp. 572-580, 2008.
- [6] S. Y. Sato, W. C. A. Pereira, and C. R. S. Vieira, "Phantom to measure displayed dynamic range at biomedical ultrasound equipments," Brazilian Journal of Biomedical Engineering, vol. 19, pp. 157-166, 2003.
- [7] A. Al-Janobi, "Performance evaluation of cross-diagonal texture matrix method of texture analysis," Pattern Recognition, v.34, n.1, pp. 171–180, 2001.
- [8] B. S. Garra, B. H. Krasner, S. C. Horii, S. Ascher, S. K. Mun and R. K. Zeman, "Improving the distinction between benign and malignant breast lesions: The value of sonographic texture analysis," Ultrasonic Imaging, v.15, n.4, pp. 267–285, 1993.